J. Phys.: Condens. Matter **8** (1996) 913–925. Printed in the UK

Computer simulation of a quadrupolar glass

M H Müser

Institut für Physik, Johannes Gutenberg-Universität, KoMa 331, D-55099 Mainz, Germany

Received 24 November 1995

Abstract. A model of solid solutions of $Ar_{1-x}(N_2)_x$ has been studied by Monte Carlo techniques over a wide range of temperatures for various concentrations x. The results are discussed in terms of a recently presented discrete-state model for cubic orientational glasses. Comparison is made to experiment. At temperatures smaller than the fcc–$Pa3$ transition temperature of the pure N_2 model system, the following phases were found. For $x > 0.9$, the $Pa3$ structure turns out to be stable. At $x = 0.9$, the $Pa3$ structure is stable, as is a frozen-in orientational disordered phase, which has a local ferroelastic type of ordering. At $x = 0.7$, indications of two-step relaxation can be observed, indicating a primary and a secondary relaxation. The local order is ferroelastic but the disorder is no longer frozen in. For smaller N_2 concentrations, $0.1 < x < 0.5$, neighbouring molecules remain parallel but the relaxation is clearly a one-step process. When translation–rotation coupling is suppressed by keeping the atoms and molecules fixed to their lattice sites, the $Pa3$ structure remains stable even at concentrations as low as $x = 0.5$.

1. Introduction

Orientational glass phases are characterized by frozen-in disorder of the orientational degrees of freedom, while the translational degrees of freedom form a crystal. An orientational glass phase can be obtained experimentally by cooling down solid mixtures of molecules and atoms such as $Ar_{1-x}(N_2)_x$ or $K(CN)_xBr_{1-x}$ if the concentration x and the pressure p are chosen appropriately. For a review of the experimental work see [1].

From a theoretical point of view, the study of orientational glasses is appealing mainly for two reasons. (i) Contrary to what is the case for canonical glasses, it is possible to approximate a microscopic model Hamiltonian H in terms of microscopic Taylor expansion coefficients like, e.g., displacement variables. This type of approach was worked out in particular by Michel and co-workers [2, 3]. Unfortunately, statistical averages of observables and the partition function $Z(\beta) = \mathrm{Tr}\{\exp(-\beta H)\}$ cannot be evaluated without making considerable simplification. (ii) There exists an analogy to the Potts glass, which has been principally promoted by Goldbart and Sherrington [4]. Exploiting this analogy, a mean-field Hamiltonian can be defined and $Z(\beta)$ can be calculated with the replica trick [5]. This kind of approach, however, lacks the mapping of a realistic microscopic Hamiltonian to the Potts glass. For a review on the theoretical work on orientational glasses see [6].

The Taylor expansion coefficients in a microscopic treatment of quadrupolar glasses are the translational displacement variables u_i^α and the local quadrupolar tensors $f_i^{\alpha\beta} = n_i^\alpha n_i^\beta - \frac{1}{3}\delta^{\alpha\beta}$, where $\delta^{\alpha\beta}$ is the Kronecker symbol, $\alpha, \beta = 1, 2, 3$, and n_i^α is the Cartesian component of the unit vector describing the orientation of a molecule at the lattice point i [3, 6]. In the case of a mixture containing only atoms and linear molecules with inversion

0953-8984/96/080913+13$19.50

symmetry, the minimum-expansion expression of the total potential V_t is therefore

$$V_t = V_0 + \sum_{ij} \left(\sum_{\alpha\beta\gamma\delta} A_{ij}^{\alpha\beta\gamma\delta} f_i^{\alpha\beta} f_j^{\gamma\delta} + \sum_{\alpha\beta\gamma} B_{ij}^{\alpha\beta\gamma} f_i^{\alpha\beta} u_j^{\gamma} + \sum_{\alpha\beta} C_{ij}^{\alpha\beta} u_i^{\alpha} u_j^{\beta} \right) \tag{1}$$

where the constant potential V_0 and the expansion coefficients $A_{ij}^{\alpha\beta\gamma\delta}$, $B_{ij}^{\alpha\beta\gamma}$, $C_{ij}^{\alpha\beta}$ depend on the given frozen-in positional disorder. The first term in the sum in equation (1) refers to the rotation–rotation coupling (RRC) for $i \neq j$ and to the crystal-field coupling (CFC) for $i = j$. The two remaining terms express the translation–rotation coupling (TRC) and the translation–translation coupling (TTC) respectively.

In this microscopic view, the interaction that changes most dramatically when a molecule is replaced by an atom at a given lattice site is the RRC which completely drops out. All of the other coefficients should remain nearly constant since the two chemical components have to be miscible. In the case of (para-H_2)$_{1-x}$(ortho-H_2)$_x$, which falls into the same class of orientational glasses as $Ar_{1-x}(N_2)_x$, the coefficients $A_{ii}^{\alpha\beta\gamma\delta}$, $B_{ij}^{\alpha\beta\gamma}$, $C_{ij}^{\alpha\beta}$ remain identical, while $A_{ij}^{\alpha\beta\gamma\delta} = 0$ if at least one of the two particles at lattice sites i and j is an ortho-H_2, which plays the role of the isotropic Ar atom.

For fcc-$Ar_{1-x}(N_2)_x$ mixtures the following extreme cases are obtained: in the dilute limit, a N_2 molecule has its preferred orientations parallel to one of the three principal axes due to CFC [7], while in the pure system, $x = 1$, the N_2 molecules are oriented along the space diagonals due to RRC [8]. Thus, the competition between CFC and RRC plays an important role.

In Potts glasses, the competing interactions are modelled by randomly distributed coupling constants J_{ij} coupling the Potts spins $\boldsymbol{S}_i$ and $\boldsymbol{S}_j$. One of the components of a Potts spin is one, and all of the other components are zero. Introducing a random field $\boldsymbol{h}_i$ at lattice site i the Hamiltonian of the Potts model is given by [9]

$$H_p = \sum_{ij} J_{ij} \boldsymbol{S}_i \cdot \boldsymbol{S}_j + \sum_i \boldsymbol{h}_i \cdot \boldsymbol{S}_i . \tag{2}$$

The appropriate choice of the distributions for J_{ij} and $\boldsymbol{h}_i$ depends on the system under consideration. The analogy between a Potts spin and the orientation of a molecule in a (mixed) crystal is due to high local energy barriers that make the orientations of the molecules quasi-discrete. Hence, the orientational state of a molecule can be described by a pseudo-Potts spin. In a semi-microscopic model [10], these pseudo-Potts spins can be coupled bilinearly to elastic variables. Structural changes and anomalies in the elastic moduli have been obtained in good qualitative agreement with experiment.

In a recent work [11], a similar approach led to a self-consistency equation for the order parameter from which the shear modulus C_{44} follows. This approach is made especially for the description of cubic orientational glasses.

It is not clear whether the analogy between Potts glasses and orientational glasses can be justified. Computer simulation is an excellent tool for investigating the assumptions made in theoretical model building. Tadič *et al* assumed in their model for cubic quadrupolar glasses that the molecules align preferentially parallel to one of the {111} axes. This assumption is in accordance with computer simulation results for $(KBr)_{1-x}(KCN)_x$ for $x = 0.75$ [12]. However, on lowering x, the correlation between the space diagonals and the orientation of the molecules might decrease.

Another open question concerns the dynamics of the freezing process. In a simple model of orientational glasses [13], a time-scale separation between primary (global) and secondary (local) relaxations has been predicted. In this work, local relaxation processes like thermally activated inversion flips of the N_2 molecules are made responsible for the anomalies in the low-temperature specific heat.

From the known experimental data, no primary and secondary relaxation could be deduced for $Ar_{1-x}(N_2)_x$. Unfortunately, there are no long-time simulations of realistic models that could be used to elucidate this question. Either the models studied were highly phenomenological [14, 15], or the correlation functions were averaged over just a few 1000 molecular dynamics steps [12, 17]. In such a short computer simulation it is clearly impossible to find a time-scale separation. In [18], much longer runs (up to 10^6 MC steps) were performed for fcc-$Ar_{1-x}(N_2)_2$, $x = 0.33$ and $x = 0.67$, from which correlation functions (10^5 MC steps long) could be deduced. For the temperatures investigated the relaxation process was clearly a one-step process. No time-scale separation in the relaxation could be observed. However, it is conceivable that the large jump from $x = 0.33$ to $x = 0.66$ or the large jumps in temperature of at least 5 K concealed the time-scale separation. Concentration-dependent studies where x varies only smoothly could reveal this result.

An important advantage of computer simulation is that all parameters are controllable. Interactions can even be switched on or off. TRC and TTC can be suppressed if the translational degrees of freedom are not moved during a Monte Carlo run. With such a procedure it is possible to investigate the influence of these interactions on the order parameter and on correlation functions.

The outline of this paper is as follows: in section 2 the model system for $Ar_{1-x}(N_2)_2$ is presented and its applicability to real systems is discussed. The observables are defined before the mean-field theory of Tadič *et al* [11] (MFT) is briefly described. In section 3 the results of computer simulations are presented and comparison is made to MFT and experiment. First, recently obtained values for the order parameter as a function of concentration x and temperature T are interpreted in terms of MFT. Predictions for the elastic constants are made. For these purposes, a self-consistent integral equation for the order parameter had to be solved. The local arrangements of the N_2 orientations are investigated. This is especially interesting as regards testing the input assumptions of the MFT. The effect of TRC and TTC on some self-correlation functions and on the phase diagram is discussed. A summary and a concluding discussion are given in section 4.

2. Methods

2.1. The model system

Our model system for the $Ar_{1-x}(N_2)_x$ mixtures consists of point atoms and linear molecules containing two force centres. The 500 atoms and molecules are initially distributed at random on a fcc lattice. Cubic periodic boundary conditions are chosen. The lattice constant a is interpolated linearly with x between the lattice constants a_{Ar} and a_{Pa3}, minimizing the classical potential energy of the pure Ar system and the classical potential of the pure N_2 system in the $Pa3$ phase, respectively. If not mentioned otherwise, the initial orientations of the N_2 molecules have been set up according to the $Pa3$ phase.

The interaction between the particles takes place via Lennard-Jones potentials:

$$V(r) = 4\varepsilon\left(\frac{\sigma}{r}\right)^6\left\{\left(\frac{\sigma}{r}\right)^6 - 1\right\}. \tag{3}$$

The potential parameters [16] have already been used by Klee *et al* yielding a very rough estimate of the phase boundaries of the $Ar_{1-x}(N_2)_x$ mixed crystal in the T–x plane [17].

The sampled variables are the centre-of-mass coordinates of all of the atoms and all of the molecules, as well as the orientational coordinates of the molecules.

This choice of potential parameters results in a fcc–$Pa3$ transition temperature $T_1 = 17.5$ K, while experimentally $T_1 \approx 35$ K [18]. Taking into account electrostatic interactions between N_2 molecules leads to a more precise phase diagram [8]. Results on solid nitrogen using more realistic potentials will be published elsewhere [19]. Note that the physical interpretation does not change if the interatomic potentials are modified in this way. In both cases we are dealing with a Hamiltonian which can be approximated by an expansion of the type mentioned in equation (1). Hence, typical experimental findings for orientational glasses [20] could be obtained within this model, e.g. the slowing down of the reorientation and the broad non-uniform distribution of local orientational order parameters smoothly evolving with temperature. The efficiency of the algorithm (measured in MC sweeps per second) decreases by nearly a factor of ten if electrostatic interactions are taken into account in the pure N_2 system. Hence, mixtures with high N_2 concentrations could no longer be equilibrated satisfactorily.

Clearly, it is conceivable that the topology of the phase diagram changes when the interactions are altered. This might happen in analogy to the noble gases where a solid phase for He does not exist at normal pressures because the de Boer parameter is too large [21]. Nevertheless, it is important to investigate various classes of phase diagrams for orientational glasses in order to understand the freezing-in process of the orientational degrees of freedom.

2.2. Observables

A very important observable for orientational glasses is the order parameter q_{EA}, which is defined in analogy to the Edwards–Anderson order parameter of spin glasses [6]. q_{EA} can be calculated by taking the limit $t \to \infty$ of the disorder-averaged function $g_i(t)$:

$$q_{EA} = \lim_{t\to\infty} \left[g_i(t)\right]_{av} \tag{4}$$

where $g_i(t)$ is a time autocorrelation function of the ith quadrupolar tensor $f_i^{\alpha\beta}$ (defined in the introduction) [6]:

$$g_i(t) = \frac{3}{2} \sum_{\alpha,\beta} \langle f_i^{\alpha\beta}(t') f_i^{\alpha\beta}(t+t') \rangle_{t'}. \tag{5}$$

q_{EA} measures the orientational localization of the molecules. From the curvature of the relaxation function $g(t) = [g_i(t)]_{av}$ insight into the relaxation processes can be obtained. The broader the relaxation function the more collective is the relaxation.

MC data at long times can be given a dynamical interpretation because importance Monte Carlo sampling amounts to time averaging along the stochastic trajectory describing a numerical realization of a Markovian master equation [22]. Comparing orientational correlation functions obtained by molecular dynamics [23] and by Monte Carlo [7] methods shows that one MC step approximately corresponds to 10^{-13} s of real time for the model system under consideration in the dilute limit. Clearly, this scale factor concerns only thermally activated processes and is not appropriate for the description of librational motion. Furthermore, the scale factor is presumably concentration dependent.

The local order of the N_2 orientations is described by the distribution function

$$P(d,x) = \left\langle \delta(|\boldsymbol{R}_i - \boldsymbol{R}_j| - d)\,\delta(\boldsymbol{n}_i \cdot \boldsymbol{n}_j - x)\right\rangle. \tag{6}$$

Here, $\boldsymbol{n}_i \cdot \boldsymbol{n}_j$ is the scalar product of two vectors indicating the orientations of the molecules at lattice sites i and j which are separated by a distance $d = |\boldsymbol{R}_i - \boldsymbol{R}_j|$. For simplicity, the values of d are replaced by those values that would have been obtained if the atoms and molecules had been constrained to their ideal fcc-lattice positions. This makes the values of d discrete and the function $P(d, x)$ easier to evaluate.

2.3. Mean-field theory

In this subsection the mean-field theory for cubic orientational glasses presented by Tadič *et al* [11] is briefly presented. One of their basic assumptions is that at low temperatures the molecules align (nearly) parallel to one of the four space diagonals, as is the case in pure N_2 solids at low pressures and low temperatures. The orientational state of the molecule at lattice point i can then be described by a symmetry-adapted number $Z_{i\mu}$ with $\mu = 1, \ldots, 3$ and $Z_{i\mu} = -1, 0$ or 1. Disorder is introduced by defining random interactions J_{ij} and random fields $h_{i\mu}$, so the phenomenological quadrupole–quadrupole interaction V_Q is given by

$$V_Q = \sum_{\mu=1}^{3} \left(\sum_{ij} J_{ij} Z_{i\mu} Z_{j\mu} + \sum_{i} h_{i\mu} Z_{i\mu} \right). \tag{7}$$

J_{ij} and $h_{i\mu}$ are Gaussian-distributed variables with the first and seconds moments $(J_0/N, J/\sqrt{N})$ and $(0, \Delta)$ respectively, N being the number of particles. Note that every molecule interacts with every other molecule with the same distribution irrespective of distance, and hence the moments are suitably scaled with N.

Starting from a Hamiltonian $H = V_Q$ the following self-consistent equations for the order parameter

$$q = \frac{1}{3} \sum_{\mu} \langle p_\mu^2 \rangle$$

have been obtained for the isotropic replica-symmetric case in the absence of long-range order and external field:

$$\begin{aligned} \langle p_\mu^n \rangle &= \int \prod_{\nu=1}^{3} \left[\frac{\mathrm{d}x_\nu}{\sqrt{2\pi}} \right] p_\mu^n \exp\left(-\frac{1}{2} \sum_{\nu} x_\nu^2 \right) \\ p_\mu &= \left(\tanh(\beta H_\mu) - \prod_{\nu \neq \mu} \tanh(\beta H_\nu) \right) \bigg/ \left(1 - \prod_{\nu} \tanh(\beta H_\nu) \right) \\ H_\mu &= J \sqrt{\langle p_\mu^2 \rangle + \tilde{\Delta}}\, x_\mu \end{aligned} \tag{8}$$

with $\tilde{\Delta} = \Delta/J^2$.

The coupling of the rotational to the translational degrees of freedom is carried out in analogy to equation (1). If only long wavelengths are concerned, it is sufficient to bilinearly couple the rotational degrees of freedom to the strain tensor components $\varepsilon_{\alpha\beta}$:

$$V_{QT} = \gamma \sum_{i} \sum_{\mu=1}^{3} Z_{i\mu} \varepsilon_{i,\mu+3} \tag{9}$$

where γ is a coupling constant and $\varepsilon_{i,\mu+3}$ the $(\mu + 3)$th component of the strain tensor in Voigt notation at lattice site i.

As in other cases where long-range order is absent, the following temperature dependence of the elastic modulus (here C_{44}) is obtained:

$$C_{44}(T) = \frac{C_{44}^0}{1 + \tilde{\gamma}\beta(1 - q)} \tag{10}$$

where C_{44}^0 is the bare shear elastic constant and $\tilde{\gamma}^2 = \gamma^2/C_{44}^0$. The bare elastic constants are given by the pure translation–translation coupling, which is not given here explicitly.

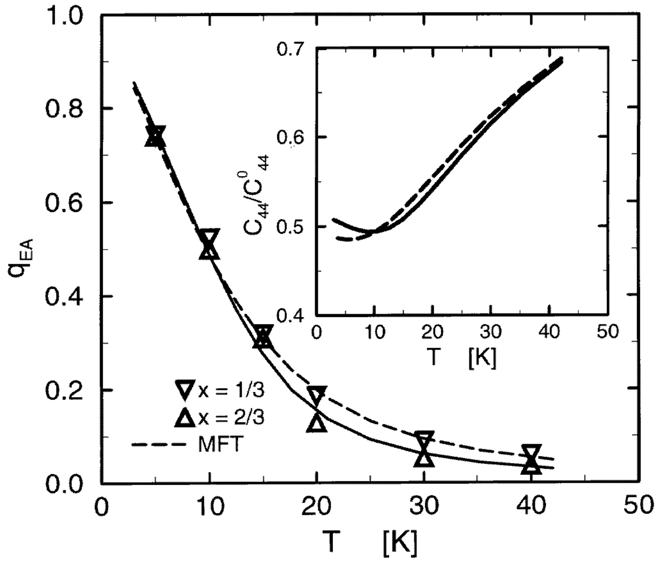

Figure 1. The order parameter $q_{EA}(T) = [\sigma]_{av}$ as a function of temperature. Symbols are simulation results [18]; lines are a fit according to a mean-field theory [11]. Inset: the relative shear elastic modulus C_{44}/C_{44}^0 according to $q_{EA}(T)$ and mean-field theory.

3. Results

3.1. The order parameter

The self-consistency equation for the order parameter obtained via the mean-field theory (MFT) presented in the last section has not yet been tested against experiment or computer experiment. Some data suitable for such a test might be the order parameter $q_{EA}(x, T)$ which has been computed recently for $x = \frac{1}{3}$ and $x = \frac{2}{3}$. The results are shown in figure 1. The lines which are obtained according to equation (8) yield good agreement within the statistical error bars. The following parameters have been used for the solid lines: (i) $x = \frac{1}{3}$, $J = 9.8$, $h = 0.9$; (ii) $x = \frac{2}{3}$, $J = 13.2$, $h = 0.28$.

The nearly quantitative agreement between simulation and mean-field theory could indicate that the four-state Potts glass with random bonds and random fields might be suitable for the description of cubic quadrupolar glasses. However, the replica-symmetric solution with the parameters given above becomes unstable at $T \approx 12$ K for $x = \frac{1}{3}$ and $T \approx 15$ K for $x = \frac{2}{3}$.

One might also argue that the S-like curvature of the order parameter is of general nature and therefore $q(T)$ might be described by any Potts model. In our opinion, the order parameter alone will not suffice for judging the relative merits of various approximative theories, and a more detailed analysis of various other quantities is required.

Tadić *et al* related the order parameter to the shear modulus C_{44}; see equation (10). This relationship between the elastic modulus and the order parameter does not depend on the specific model but rather is a general feature of the bilinear coupling of orientational degrees of freedom and translational degrees of freedom, as long as long-range order is absent.

Good qualitative agreement with experiment and with theory is found: the higher the concentration of the molecules, the higher is the temperature where the minimum in C_{44} is found. According to provisional experimental data [24], there is even a good quantitative agreement. A slight minimum in $C_{11} + 2C_{12}$ at a temperature $T \approx 20$ K is observed by using Raman scattering techniques for $x = 0.4$.

It is worth mentioning that the systems were in thermal equilibrium at the temperatures where the proposed minima in C_{44} occur. This means that the minimum in C_{44} does not coincide with a (glass) transition temperature because in this case the correlation times would diverge, and therefore an equilibration would not have been possible using standard MC methods. Hence, if there is a characteristic freezing temperature where correlation times and correlation lengths diverge, it must be lower than the temperature where the minimum in C_{44} occurs. Note that the mean-field theory quoted above would imply for $h = 0$ a transition at finite temperatures, while in the short-range case [9] there is no transition at all.

3.2. *Local ordering*

Experimentally, it is difficult to determine the correlation between the orientations of neighbouring molecules in orientationally disordered systems. However, this information might be important for understanding the freezing-in process of the orientational degrees of freedom. In a computer simulation study such correlations can be quantified by measuring $P(d, x)$ as defined in equation (6).

For $Ar_{1-x}(N_2)_x$ mixtures, a short-range order similar to the order in the $Pa3$ symmetry is suspected to appear in an intermediate-concentration range $x \approx 0.5$ where experimentally $Ar_{1-x}(N_2)_2$ crystallizes in the fcc symmetry [25]. Such a local ordering can be visualized by computing $P(d, x)$.

In figure 2 the results for $P(d, x)$ are presented for Lennard-Jones $Ar_{1-x}(N_2)_x$ mixtures. For the pure N_2 crystal, $P(d, x)$ is shown 10% above and 10% below the transition temperature obtained, T_1. For $T > T_1$, the orientations of neighbouring molecules are nearly equally distributed. For $T < T_1$, a maximum in $P(d, x)$ can be observed at $x = 1/3$ for the nearest neighbours and for the third-nearest neighbours, according to the $Pa3$ structure. The next-nearest neighbours and the fourth-nearest neighbours belong to the same sublattice as the central N_2 molecule and therefore a peak at $x = 1$ is observed in $P(d, x)$.

In the mixed cases, neighbouring molecules preferentially align parallel to each other. The length of the ferroelastic domains arising obviously increases with increasing N_2 concentration. Note that for $Ar_{0.33}(N_2)_{0.67}$, a relative minimum exists in the distribution function $P(d, x)$ at $x \approx 0.75$. The minimum becomes all the more pronounced as the distance d increases. This observation is not easy to explain, but it shows that locally the ferroelastic domain length scale is not the only characteristic length scale.

The correlation of the average molecular axis to one of the three principal axes $\{100\}$ of the cubic system and to one of the four space diagonals $\{111\}$ has been determined as well. At $T = 10$ K, we obtain $q_{100} = 0.33$ and $q_{111} = 0.25$ for $Ar_{0.67}(N_2)_{0.33}$. For $Ar_{0.33}(N_2)_{0.67}$, $q_{100} = 0.22$ and $q_{111} = 0.32$ is obtained at the same temperature. Hence, the higher the N_2 concentration the more pronounced is the correlation with one of the space diagonals. Nevertheless, there is no dramatic difference between the correlations.

For $Ar_{0.1}(N_2)_{0.9}$, both types of local orientational order can be observed. Ferroelastic

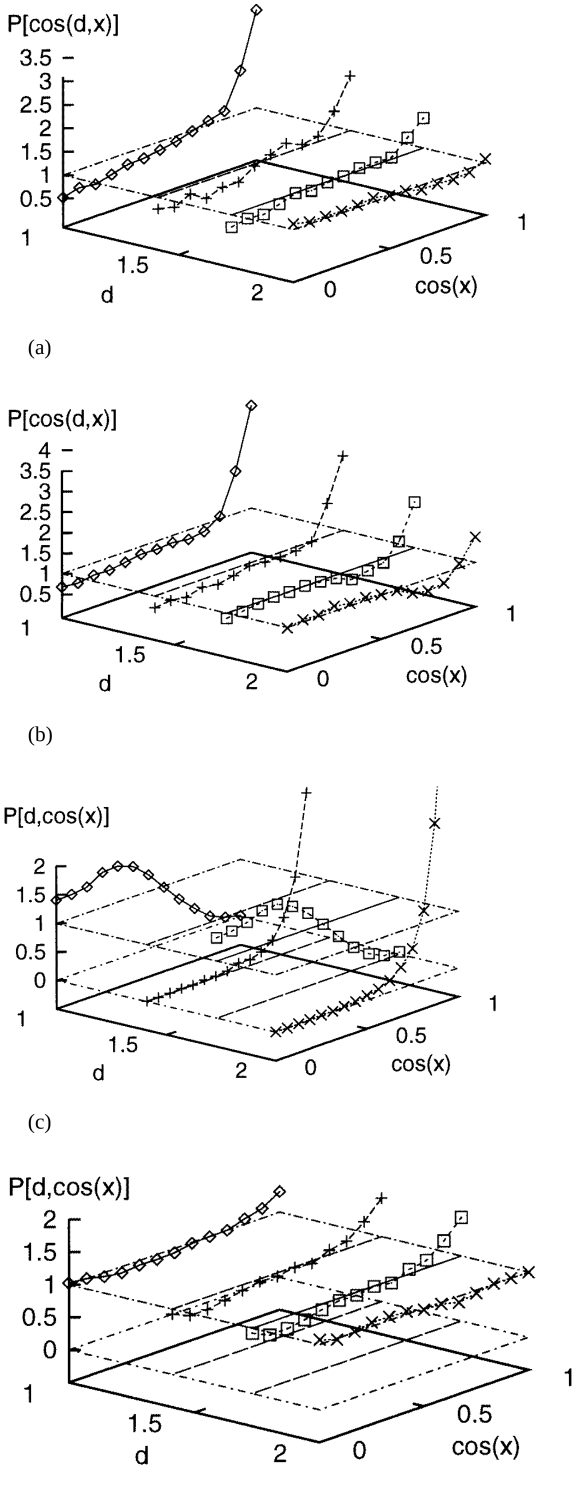

(a)

(b)

(c)

(d)

Figure 2. The angle–angle correlation function of N_2 molecules. (a) $x = 1/3$, $T = 10$ K, (b) $x = 2/3$, $T = 10$ K, (c) $x = 1$, $T = 19$ K, (d) $x = 1$, $T = 16$ K. The grid shows the *a priori* distribution.

ordering is obtained by cooling this mixture down. In this case, all molecules align parallel to one of the {111} axes, resulting in a trigonal-like phase. However, for temperatures $T < T_1$, the $Pa3$ structure remains stable if the initial structure corresponds to the $Pa3$ symmetry.

The results presented in this subsection might be altered if more realistic potentials were used. In particular, one expects a stronger tendency of neighbouring molecules to align perpendicularly if electrostatic interactions are taken into account. Nevertheless, the study presented starts from a microscopic Hamiltonian and it is quite possible that other real mixtures of atoms and molecules fall into the class of Lennard-Jones $\mathrm{Ar}_x(\mathrm{N}_2)_{1-x}$.

3.3. *Time correlation functions*

Primary and secondary relaxations have not yet been observed for $\mathrm{Ar}_{1-x}(\mathrm{N}_2)_x$ mixtures, while two-step relaxation is quite common in other classes of disordered materials.

Experimentally, the orientation-density self-correlation function is difficult to obtain because the homonuclear N_2 molecules do not couple to the dielectric permittivity.

Hence, computer simulation is the appropriate tool for investigating correlation functions of the type of equation (5). In order to perform well-defined averaging, good equilibration has to be performed.

The duration of equilibration depended on the concentration. The most extensive studies were carried out for $x = 0.7$, a sample of 500 particles in total, which was equilibrated for 10^6 MC steps. The correlation function for this sample was then averaged over 2×10^6 MC steps. This corresponds to 150 h of CPU time on a CRAY Y-MP. The computational effort for the study of the $x = 0.5$, $x = 0.6$ and $x = 0.8$ samples was in the same range.

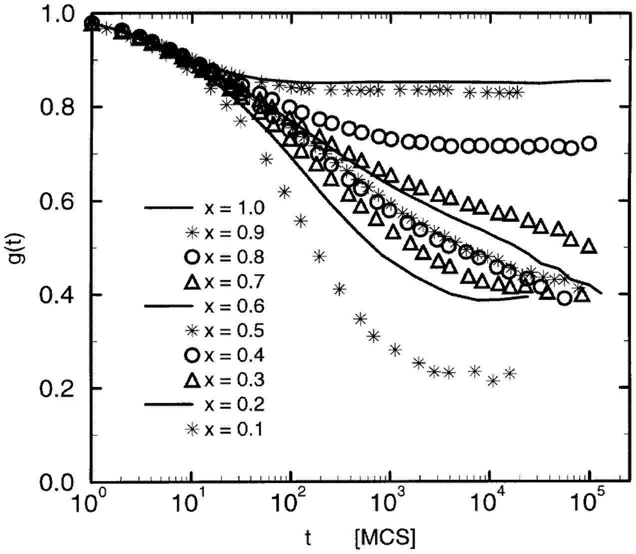

Figure 3. The correlation function $g(t)$ for various N_2 concentrations x at $T = 12$ K.

In figure 3, the orientation correlation function is shown for $x = 0.1, 0.2, \ldots, 1.0$ at the constant temperature $T = 12$ K. The correlation time obviously increases with the N_2 concentration x. A clear plateau at MC times $t = 10^5$ in the self-correlation function can only be obtained for $x \leqslant 0.3$. Note that the order parameter which is given by the correlation function at times $t \to \infty$ first increases with x up to $x = 0.3$ and then seems to decrease with increasing x. In the range $0.4 \leqslant x \leqslant 0.7$, only an upper bound can be given for the order parameter. For concentrations $x \geqslant 0.8$, a clear plateau can be found again in $g(t) = [g_i(t)]$ at MC times $t \geqslant 10^2$ MC steps. The corresponding plateau values can again be interpreted as the order parameter provided that with increasing particle number the plateau stabilizes for infinite times.

An interesting feature of figure 3 is that the relaxation is clearly a one-step procedure at low concentrations. With increasing x, however, the relaxation begins to be broadened. At $x = 0.7$, strong indications for a two-step relaxation are found with a primary relaxation for $t > 10^4$ and a secondary relaxation for $t < 10^3$. Unfortunately, this is not a real-time scale separation, but nevertheless it is enough to show up as a shoulder in the relevant correlation function.

3.4. Translation–rotation coupling

The translation–rotation coupling (TRC) plays an important role when the generalized susceptibility is determined experimentally by measuring the elastic constants [6]. On the other hand, TRC induces changes in the Bravais lattice due to the onset of orientational ordering or freezing [3]. One could now ask the opposite question—of what the consequences of TRC are for the orientational ordering.

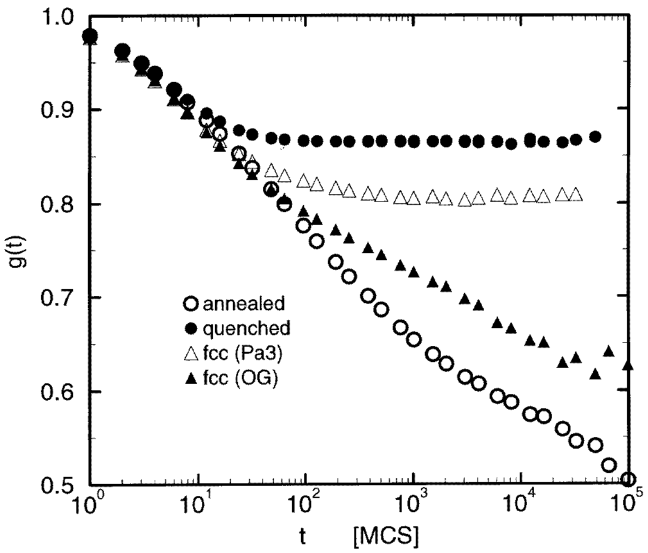

Figure 4. The correlation function $g(t)$ for $x = 0.7$ at $T = 12$ K. Different algorithms have been used; see the text.

Different forms of simulation algorithms were used to elucidate this question and the resulting self-correlation functions for $x = 0.7$ and $T = 12$ K are shown in figure 4:

(i) *annealed:* all degrees of freedom are moved;

(ii) *quenched:* the translational degrees of freedom are constrained to their thermal equilibrium positions;

(iii) *fcc* ($Pa3$): the translational degrees of freedom are constrained to the ideal fcc positions; the initial configuration of the orientational degrees of freedom corresponds to the $Pa3$ symmetry;

(iv) *fcc* (OG): for the translational degrees as in (iii); the initial configuration of the orientational degrees of freedom is taken from case (i).

In all cases at least 3×10^5 MC steps of equilibration were performed before the observables were averaged.

Although translational displacement variables are considered to be small, the four cases investigated yield quite different forms of relaxation functions and local orientational ordering.

In case (i), the orientation correlation function has the lowest values at every time investigated. If the translational degrees of freedom are then fixed to their thermal equilibrium positions, case (ii), a clear plateau in $g(t)$ can be found very quickly, while for times $t < 10$ the two relaxation functions are similar. Thus, for 'successful' reorientational motion it is important that the local fields acting on the orientations of the molecules fluctuate in time. Static local fields in the form of a frozen-in TRC favour an unrealistically high order parameter.

In the cases (iii) and (iv), the translational degrees of freedom were set up according to the fcc symmetry, so here the TRC is completely suppressed. When initially started with a $Pa3$-symmetry-type ordering of the orientational degrees of freedom, case (iii), the system does not 'forget' the initial configuration. In the case of a disordered starting configuration taken from case (i), neighbouring molecules preferentially align parallel as in case (i)—however, resulting in a slightly enhanced order parameter and with a much less pronounced two-step relaxation. Even though for finite systems no difference between zero-field-cooled and field-cooled cases exists, it turns out that between the '$Pa3$-field-cooled' configuration, case (iii), and the 'zero-field-cooled' configuration, case (iv), a large energy barrier exists that cannot be surmounted within a large number of MC steps. This, however, is possible if smaller samples containing 108 particles in total are considered. One can conclude that the barrier increases with system size and hence, in infinitely large systems, the barrier separating the (meta-)stable states becomes infinitely large. Note that the '$Pa3$-field-cooled' mixture loses its memory within approximatively 100 MC steps as soon as the TRC is switched on again.

4. Discussion and conclusions

Lennard-Jones $Ar_{1-x}(N_2)_x$ mixtures have been studied with Monte Carlo techniques over a wide range of temperature and N_2 concentrations x. The main points investigated in this paper are the analogy between Potts glasses and orientational glasses, the local orientational ordering, the stochastic dynamics of reorientational motion and the influence of the translation–rotation coupling (TRC) on the phase diagram.

The mean-field theory (MFT) of the four-state Potts glass in three dimensions of Tadič *et al* [11] describes the order parameter $q(T)$ for $x = 0.33$ and $x = 0.67$ well, if its parameters are suitably adjusted. However, the replica-symmetric solution becomes unstable at relatively low values for $q(T)$, so the good agreement between theory and simulation is not yet really satisfactory. The strong effects of TRC on the properties (figure 4) indicates that models such as that of equation (2), which do not include TRC effects on the Potts spins themselves, are not really adequate for our system, at least if dynamic quantities are considered. Using the MFT, nevertheless, a minimum in the elastic modulus C_{44} can be deduced at temperatures $T \approx 10$ K in agreement with experimental data. However, the anomaly has been observed in $C_{11} + 2C_{12}$. This might be due to the fact that the molecules do not only align parallel to the space diagonals but also align parallel to the cubic main axes, contrary to the MFT assumptions.

Nevertheless, the study of Potts models is very promising as regards understanding static properties associated with the freezing-in process in orientational glasses. The mapping from a realistic Hamiltonian, e.g. that given in equation (1), to a Potts model Hamiltonian, given in equation (2), is one of the most important unresolved questions. In particular, it would be desirable to obtain the first and the second moments of the coupling constants J_{ij} and the random fields h_i as functions of the concentration x and the (realistic) microscopic expansion coefficients as a function of distance between the lattice sites. This is an important task for the future.

The evidence for a two-step relaxation in $\mathrm{Ar}_{1-x}(\mathrm{N}_2)_x$ mixtures is a new result which can only be found in a quite narrow range of concentration below the critical concentration x_c, where long-range order sets in. For still lower x the relaxation functions are broadened and of stretched-exponential type (see [23]), but they are clearly one-step processes. It would be interesting to know whether these findings can be reproduced in experiments by measuring the central peak. In order to provide the experimentalist with more precise information, a molecular dynamics study based on more realistic potentials would have to be performed. These studies, however, would be even more CPU time intensive than the studies presented here, because the successive configurations in molecular dynamics studies are more correlated than in MC simulations and because the use of more realistic potentials decreases computational speed by approximately a factor of ten.

Another important finding presented here is the intensity with which the TRC influences the phase diagram and the orientational correlation functions. No more significant reorientational motion is possible when the translational degrees of freedom are constrained to their thermal equilibrium positions. The constraint mentioned restricts the system to moving only in one or in a few local minima of potential energy. When the translational degrees of freedom are constrained to the ideal fcc-lattice positions, the $Pa3$ ordering becomes at least metastable even for concentrations as low as $x = 0.7$. The approach in which TRC is considered as a small field acting on the orientational degrees of freedom therefore should be revised, at least for the present system.

Acknowledgments

The author thanks R Feile, T Westerhoff and F Bruchhäuser for stimulating discussions as well as K Binder for critically reading the manuscript. The research described herein was carried out in the framework of the Sonderforschungsbereich 262 der Deutschen Forschungsgemeinschaft. This work was supported also by the Bundesministerium für Bildung, Wissenschaft, Forschung und Technologie (BMFT) No 03N8008C. The computations were carried out on the CRAY Y-MP of the HLRZ at Jülich.

References

[1] Höchli U T, Knorr K and Loidl A 1990 *Adv. Phys.* **39** 409
[2] Michel K H and Naudts J 1977 *Phys. Rev. Lett.* **39** 212
Michel K H and Rowe J M 1980 *Phys. Rev.* B **22** 1417
De Raedt A, Binder K and Michel K H 1981 *J. Chem. Phys.* **75** 2977
Michel K H 1985 *Phys. Rev.* B **35** 1405; 1986 *Phys. Rev. Lett.* **57** 2188
[3] Lynden-Bell R M and Michel K H 1994 *Rev. Mod. Phys.* **66** 721
[4] Goldbart P M and Sherrington D 1985 *J. Phys. C: Solid State Phys.* **18** 1923

[5] Binder K and Young A P 1986 *Rev. Mod. Phys.* **58** 801
[6] Binder K and Reger J D 1992 *Adv. Phys.* **41** 547
[7] Müser M H, Helbing W, Nielaba P and Binder K 1994 *Phys. Rev.* E **49** 3956
[8] Scott T A 1976 *Phys. Rep.* **27** 89
Belak J, Le Sar R and Etters R D 1990 *J. Chem. Phys.* **92** 5430
[9] Haas F F, Vollmayr K and Binder K 1996 *Z. Phys.* B at press
[10] Vollmayr H, Kree R and Zippelius A 1990 *Europhys. Lett.* **12** 235; 1991 *Phys. Rev.* B **44** 12 238
[11] Tadiĉ B, Pirc R, Blinc R, Petersson J and Wiotte W 1994 *Phys. Rev.* B **50** 9824
[12] Lewis L J and Klein M L 1989 *Phys. Rev.* B **40** 7080
[13] Sethna J P, Nagel S R and Ramakrishnan T V 1984 *Phys. Rev. Lett.* **53** 2489
Sethna J P 1986 *Phys. Today* **39** 20
[14] Hammes D, Carmesin H-O and Binder K 1989 *Z. Phys.* B **76** 115
[15] Holdsworth P C W, Gingras M J P, Bergersen B and Chan E P 1991 *J. Phys.: Condens. Matter* **3** 6679
[16] $\epsilon_{ArAr} = 121k_B$ K, $\sigma_{ArAr} = 3.40$ Å, $\epsilon_{NN} = 37.3k_B$ K, $\sigma_{NN} = 3.31$ Å, $\epsilon_{ArN} = (\epsilon_{ArAr}\epsilon_{NN})^{1/2}$, $\sigma_{ArN} = (\sigma_{ArAr}\sigma_{NN})^{1/2}$, diameter of the N_2 molecule: 0.545 Å.
[17] Klee D H, Carmesin H O and Knorr K 1988 *Phys. Rev. Lett.* **61** 1855
[18] Müser M H and Nielaba P 1995 *Phys. Rev.* B **51** 2723
[19] Löding D, Müser M H and Nielaba P in preparation
[20] Estève D, Sullivan N S and Devoret M 1982 *J. Physique Lett.* **43** 793
[21] Ashcroft N W and Mermin N D 1976 *Solid State Physics* (New York: Holt, Rinehart and Winston)
[22] Binder K (ed) 1986 *Monte Carlo Methods in Statistical Physics* 2nd edn (Berlin: Springer)
[23] Müser M H and Ciccotti G 1995 *J. Chem. Phys.* **103** 4273
[24] Bruchhäuser F and Feile R 1995 *Preprint*
[25] Hamida J A, Sullivan N S and Genio E B 1995 *Preprint*